Contents lists available at ScienceDirect

Clinical and Translational Radiation Oncology
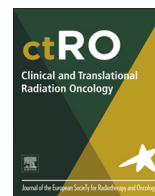
Original Research Article

Whole-ventricular irradiation for intracranial germ cell tumors: Dosimetric comparison of pencil beam scanned protons, intensity-modulated radiotherapy and volumetric-modulated arc therapy

Dora Correia [a,b,*], Dario Terribilini [c], Stefan Zepter [a], Alessia Pica [a], Nicola Bizzocchi [a], Werner Volken [c], Sonja Stieb [b], Frank Ahlhelm [d], Evelyn Herrmann [b], Michael K. Fix [c], Peter Manser [c], Daniel M. Aebersold [b], Damien C. Weber [a,b]

[a] Center for Proton Therapy, Paul Scherrer Institute, ETH Domain, Villigen, Aargau, Switzerland
[b] Department of Radiation Oncology, Inselspital, Bern University Hospital, University of Bern, Switzerland
[c] Division of Medical Radiation Physics, Inselspital, Bern University Hospital, University of Bern, Switzerland
[d] Department of Radiology, Cantonal Hospital Baden, Baden, Aargau, Switzerland

ABSTRACT

Background: Whole-ventricular radiotherapy (WV-RT) followed by a boost to the tumor bed (WV-RT/TB) is recommended for intracranial germ cell tumors (IGCT). As the critical brain areas are mainly in the target volume vicinity, it is unclear if protons indeed substantially spare neurofunctional organs at risk (NOAR). Therefore, a dosimetric comparison study of WV-RT/TB was conducted to assess whether proton or photon radiotherapy achieves better NOAR sparing.
Methods: Eleven children with GCT received 24 Gy(RBE) WV-RT and a boost up to 40 Gy(RBE) in 25 fractions of 1.6 Gy(RBE) with pencil beam scanning proton therapy (PBS-PT). Intensity-modulated radiotherapy (IMRT) and volumetric-modulated arc therapy (VMAT) plans were generated for these patients. NOAR were delineated and treatment plans were compared for target volume coverage (TVC), homogeneity index (HI), inhomogeneity coefficient (IC) and (N)OAR sparing.
Results: TVC was comparable for all three modalities. Compared to IMRT and VMAT, PBS-PT showed statistically significant optimized IC, as well as dose reduction, among others, in mean and integral dose to the: normal brain (−35.2%, −32.7%; −35.2%, −33.0%, respectively), cerebellum (−53.7%, −33.1%; −53.6%, −32.7%) and right temporal lobe (−14.5%, −31.9%; −14.7%, −29.9%). The Willis' circle was better protected with PBS-PT than IMRT (−7.1%; −7.8%). The left hippocampus sparing was higher with IMRT. Compared to VMAT, the dose to the hippocampi, amygdalae and temporal lobes was significantly decreased in the IMRT plans.
Conclusions: Dosimetric comparison of WV-RT/TB in IGCT suggests PBS-PT's advantage over photons in conformality and NOAR sparing, whereas IMRT's superiority over VMAT, thus potentially minimizing long-term sequelae.

1. Introduction

Intracranial germ cell tumors (IGCT) represent a histologically heterogeneous pediatric group of primary predominantly midline tumors of the CNS, most commonly seen in the pineal and the suprasellar region [1,2], classically divided into two main groups: germinomas – the most common –, and non-germinomatous GCT, which carry a less favorable prognosis [3,4]. Germinomas are highly sensitive to both chemotherapy and radiotherapy (RT), and curable by RT alone [1,2,4], either photons or protons [5]. They

present an excellent prognosis with overall survival of 93.7% five years after RT alone, 100% and 80.6% at 10- and 20-years, respectively [1,6,7]. Macdonald showed early clinical outcomes of IGCT patients treated with protons where local control, progression-free survival, and overall survival rates were, respectively, 100%, 95%, and 100%, at a median follow-up of 28 months [8]. Whole ventricular system irradiation followed by a boost to the tumor bed (WV-RT/TB) is considered a well-established treatment for localized germinomas{MacDonald, 2003 #259} [8].

There has been an effort for treatment de-escalation, due to: first, good response rates to neoadjuvant chemotherapy in non-disseminated disease [9], with low leptomeningeal recurrence [1]; second, noteworthy toxicity in long-term survivors [7]. However, evaluating cerebral toxicity is extremely difficult as we only begin to understand the intricate interplay between the different substructures in physiological conditions, let alone in pathological conditions [10]. Nonetheless, studies of Merchant et al. [11] demonstrated that radiation dose-volume parameters remain the most clinically significant determinants of intelligence quotient (IQ) outcomes and that further reduction in radiation dose to specific volumes of the brain should be pursued [12]. Relative to photons, hadron therapy could achieve even better protection of healthy tissues by improved beam trajectory [8], having the potential to prevent the genesis of radiogenic impairment [13], thus being expected to reduce late effects without decreasing local control and survival [5].

However, taking into account that most of the neurofunctional organs at risk (NOAR) are partly enclosed or in the direct vicinity of the target, we hypothesized that there would not be a dosimetric advantage of pencil beam scanning proton therapy (PBS-PT) over a state of the art photon treatment technique. To the best of our knowledge, no dosimetric comparison based on WV-RT/TB has yet been made between PBS-PT and photon RT for non-metastatic IGCT with focus on NOAR sparing. Therefore, we performed a planning study with the aim of determining the dosimetric difference between intensity-modulated radiotherapy (IMRT) and volumetric-modulated arc therapy (VMAT) on a cohort of IGCT patients treated with PBS-PT WV-RT/TB, using dose-volume indices of target volume coverage (TVC) and (N)OAR. Hereby, we compared the sparing potential of NOAR, currently used as a surrogate for neurocognition, cerebrovascular and neuroendocrine function, as well as other important structures, such as optic apparatus and cochleae, delineated on a routine basis for the planning of brain tumors RT.

2. Materials and methods

2.1. Patient selection

Between 2005 and 2017, 11 patients (8 males; 6–16 years, median 11) with a histologically proven diagnosis of localized IGCT were treated, after multi-agent chemotherapy, with PBS-PT at the Centre for Proton Therapy at the Paul-Scherrer Institute (PSI). They consisted of 2 bifocal germinomas, 4 pineal, 2 suprasellar, while 3 IGCT presented an atypical location with infiltrative spread within the ventricular system. Written, informed consent to the PBS-PT was obtained from the children legal guardians. Institutional review board approval was obtained before record and plan review. Complete anonymity of names and medical record numbers was maintained.

2.2. Target volume and organ at risk delineation

First, all the 11 treatment planning-CTs and pre-irradiation MRI studies were anonymized and imported into a research database of

Velocity (version 3.2.1, Varian Medical Systems, Inc., Palo Alto, USA). The MRIs were anatomically registered to the CT to facilitate volume definition. Then, for each patient, all volumes of interest (VOI) were delineated or adapted by a single radiation oncologist and reviewed by a neuro-radiation oncologist, as well as one neuroradiologist. For the purpose of this study, a 3 mm isometric margin, created on the same treatment planning software (TPS), was used for both planning treatment volumes (PTV). Delineation guidelines of the target volumes [14] and (N)OAR [15], as well as their dose constraints are detailed in the supplementary file A.

2.3. Treatment planning

The planning-CT data was sent in DICOM format, and all data transfers were made using file transfer protocol over Internet connections. The same VOI, dose prescription, and constraints were used to ensure comparability among the plans. The WV/TB were prescribed 24 Gy (PTV_Low), followed by a boost of 16 Gy to the TB (PTV_High), achieving a total dose of 40 Gy in 1.6 Gy per fraction. The plans were normalized to get 100% of the prescribed dose (D_p) as the mean dose to each PTV. All treatment plans were optimized to maximize TVC whilst sparing OAR. Besides the hippocampi and temporal lobes, no further fixed constraint was set for the NOAR than the as low as reasonably achievable (ALARA) concept [10], due to its location towards the target and lack of consensual constraints.

After trying and comparing different beam arrangements, all patients were treated with PBS-PT with three non-coplanar proton fields for both treatment series, with different gantry angulations and table rotation. Similar field arrangements have been used for the first phase and an adapted one for the boost (example in Fig. 1): one posterior field (G180deg, couch 0), two superior oblique fields (G90deg, couch 315–325 and G270deg, couch 35–45), in IEC61217 coordinate convention. All PBS-PT cases were planned with single field uniform dose, using the PSIPlan TPS (version 2.9.1-exp). The generic relative biologic effectiveness (RBE) factor for protons of 1.1 (relative to ^{60}Co) was utilized, and proton dose was expressed in terms of Gy(RBE) (i.e., Gy(RBE) = proton physical Gy × 1.1) [16]. The ion source was a dedicated 250 MeV cyclotron. Protons were actively delivered using a PBS paradigm, as previously described [17]. Individual weights of the Bragg peak were computed using a dose based optimization scheme [18] to obtain an optimal TVC. Proton dose calculation was performed using a 3D dose-calculation algorithm developed at PSI [19].

Comparison planning with IMRT and VMAT was performed on the original anonymized planning CT datasets and its respective study VOI. For the IMRT planning, after comparing with other beam arrangements, seven fields were used for the primary and five for the boost phase. The dose distribution of the photon plans was calculated with the Anisotropic Analytical Algorithm version 13.6.23, and optimized with the Dose Volume Optimizer version 11.0.31, on the Eclipse External Beam Planning (same version as described in 2.2).

2.4. Comparative evaluation of treatment plans

The proton plans were imported to Eclipse for comparison with the photon plans, where they were quantitatively assessed using dose-volume histograms (DVH) for all VOI. Dose parameters were extracted to evaluate proper TVC, assure compliance with the OAR dose constraints and determine differences between all RT modalities. TVC was assessed by the evaluation of the volume receiving a minimum of 90%, 95%, and 100% of the prescribed doses ($V_{90\%}$, $V_{95\%}$, $V_{100\%}$, respectively) [13,20]. Dose distribution in the PTV was evaluated with the homogeneity index (HI) and inhomogeneity coefficient (IC). The integral dose (ID) (Supplementary file) allows the
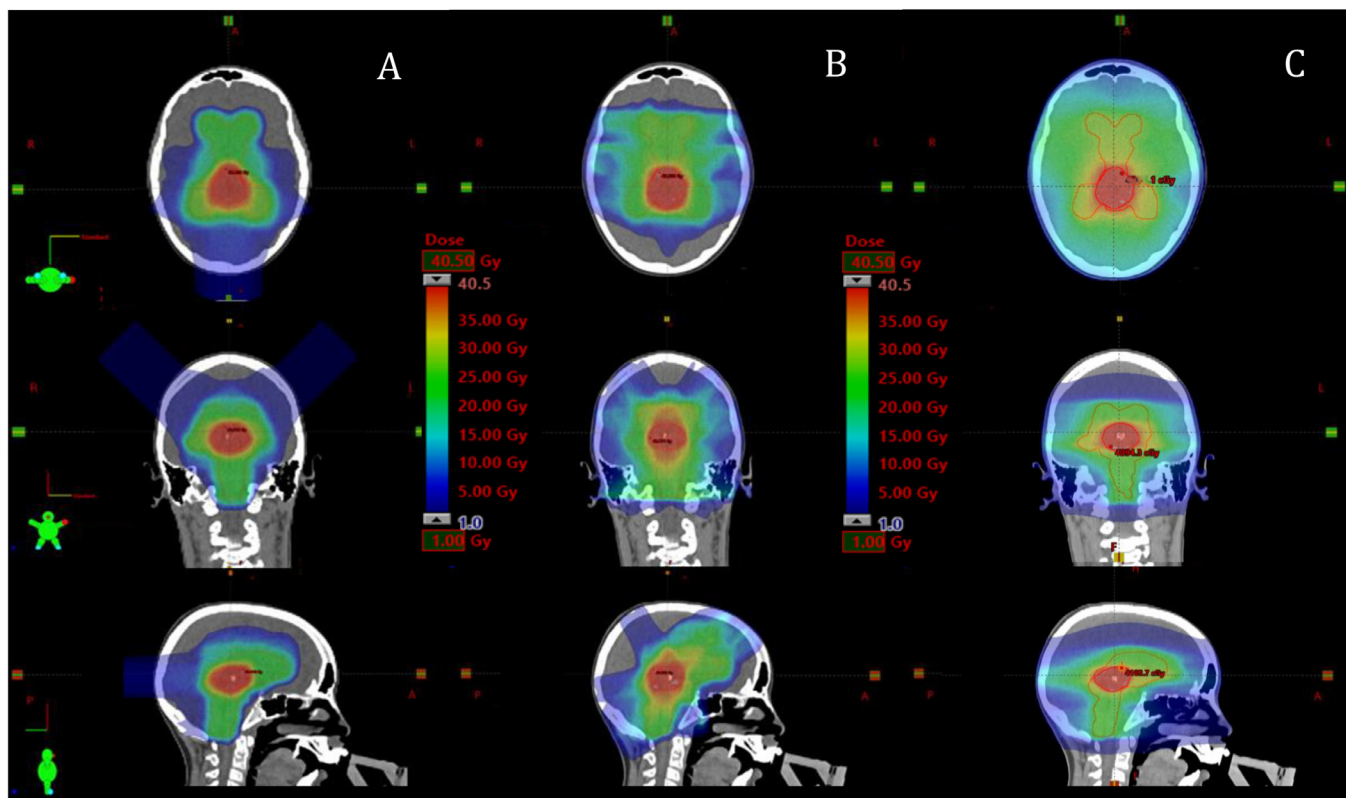
Fig. 1. Comparison of dose distribution in three different modalities for a patient with intracranial germ cell tumor: (A) Pencil beam scanning proton beam therapy (PBS-PT) plan. (B) Intensity-modulated radiotherapy (IMRT) plan. (C) Volumetric modulated arc therapy (VMAT) plan. PTV_Low is delineated in orange, PTV_High in red. (For interpretation of the references to color in this figure legend, the reader is referred to the web version of this article.)

evaluation of the lower dose spread compared to conventional measurements [21].

2.5. Statistics

Statistical analysis was performed on IBM® SPSS® Statistics software, version 24 (Armonk, NY). Descriptive statistics were used to calculate the differences in treatment parameters of proton and photon therapy. The Friedman test with the Bonferroni posttest was applied for analysis of statistically significant differences between several dosimetric parameters of the targets and (N) OAR of the proton and photon plans, with corresponding two-sided 95% confidence intervals to correct for multiple comparisons. A p-value inferior to 0.017 (Bonferroni correction) was considered statistically significant.

3. Results and discussion

3.1. Target volume coverage

Despite the normalization of each PTV (see 2.3), after extracting the DVH values automatically with an Eclipse protocol template, a technical deviation $\leq 0.25\%$ could be seen (Table 1) if performed on another TPS than where it was planned. Therefore, the PBS-PT results should be critically appraised with the same amount of uncertainty. For this reason, only higher deviations (>0.25%), statistically significant (p < 0.017), will be mentioned.

TVC was comparable for all three modalities (Fig. 2). However, PBS-PT achieved a better $V_{100\%}$ (22.5%) in PTV_High, compared to VMAT.

Comparing to IMRT and VMAT, both PTV showed with PBS-PT a higher minimum dose (D_{min}) to the PTV (PTV_Low: 26.4%, 18.2%;

PTV_High: 15.9%, 7.8%). Both IC were significantly lower for protons (PTV_Low: −50.0%, −33.3%; PTV_High: −44.8%, −30.4%), indicating a lower variability of the target dose distribution in PBS-PT than in the photon modalities.

The dose distribution homogeneity on the primary phase was optimized in the VMAT plans, as the PTV_Low HI was significantly lower than the other RT techniques, while PBS-PT was better than IMRT on the boost phase (Table 1).

3.2. Neurofunctional organ at risk sparing

For the OARs, 100% was considered to be 40 Gy (Table 1). All hard constraints were met, independently of the technique used.

3.2.1. NOAR of neurocognitive function

The hippocampal and amygdalae D_{mean} and ID seem better spared with IMRT than VMAT, while on the left hippocampus the IMRT dose sparing seems higher than with the remaining techniques (−6.2% D_{mean}, −6.1% ID than PBS-PT; −10.8% D_{mean} and ID each, comparing with VMAT). However, taking into account the hippocampal proximity to the target, its soft constraint of D40% ≤ 7.3 Gy could never be reached – its lowest absolute dose was 24.2 Gy on one PBS-PT plan.

There is growing evidence from structural and functional imaging studies that the cerebellum plays an evident role in neurocognition. Radiation to the posterior fossa has shown to have a negative effect on neurocognitive outcomes in long-term pediatric brain survivors [12]. Gan et al. described that the patient with the lowest neuropsychological scores received 36 Gy D_{max} on the cerebellum and low radiation doses on the whole brain and hippocampi [22]. In our cohort, only one case (PBS-PT) achieved a $D_{max} < 36$ Gy, otherwise, the PBS-PT average was 39.6 Gy (range,

Table 1
Comparison of target volume coverage and normal tissue sparing between PBS-PT, IMRT and VMAT.

VOI	Parameter	PBS-PT	IMRT	VMAT	PBS-PT vs. IMRT (%)	PBS-PT vs. VMAT (%)	IMRT vs. VMAT (%)
PTV_Low	D_{max} (%)	106.8 ± 1.3	107.0 ± 1.7	107.2 ± 0.8	−0.2	−0.4	−0.2
	D_{mean} (%)	100.3 ± 0.6	100.0 ± 0.0	100.0 ± 0.0	0.2	0.2	0.0
	D_{min} (%)	89.0 ± 2.0	70.4 ± 11.1	75.3 ± 10.2	26.4*	18.2*	−6.5
	Mean ID (Gy.ml)	7620.8 ± 3572.9	7608.4 ± 3578.9	7608.4 ± 3578.9	0.2	0.2	0.0
	Coverage						
	$V_{90\%}$ (%)	99.9 ± 0.0	99.7 ± 0.0	99.9 ± 0.0	0.2*	0.0	−0.2
	$V_{95\%}$ (%)	99.1 ± 0.0	98.7 ± 0.0	99.3 ± 0.0	0.4	−0.2	−0.6
	$V_{100\%}$ (%)	63.9 ± 0.1	59.7 ± 0.2	55.2 ± 0.0	7.0	15.8	8.2
	Dose distribution						
	HI	4.9 ± 0.5	5.5 ± 1.5	3.5 ± 0.6	−10.9	40.0*	57.1*
	IC	0.2 ± 0.0	0.4 ± 0.1	0.3 ± 0.1	−50.0*	−33.3*	33.3
PTV_High	D_{max} (%)	104.7 ± 1.6	105.8 ± 2.1	106.1 ± 1.5	−1.0	−1.3	−0.3
	D_{mean} (%)	100.1 ± 0.1	100.0 ± 0.0	100.0 ± 0.0	0.1*	0.1*	0.0
	D_{min} (%)	89.4 ± 2.8	77.1 ± 7.4	82.9 ± 3.9	15.9*	7.8*	−7.0*
	Mean ID (Gy.ml)	1909.1 ± 2346.4	1907.4 ± 2345.1	1907.4 ± 2345.1	0.1*	0.1*	0.0
	Coverage						
	$V_{90\%}$ (%)	99.7 ± 0.0	99.3 ± 0.0	99.9 ± 0.0	0.4	0.2	−0.6
	$V_{95\%}$ (%)	98.4 ± 0.0	93.5 ± 0.2	98.2 ± 0.0	5.2	0.2	−4.8
	$V_{100\%}$ (%)	70.8 ± 0.1	55.9 ± 0.2	57.8 ± 0.0	26.7	22.5*	−3.3
	Dose distribution						
	HI	4.7 ± 1.0	6.4 ± 1.2	5.0 ± 1.4	−26.6*	−6.0	28.0
	IC	0.2 ± 0.0	0.3 ± 0.1	0.2 ± 0.0	−44.8*	−30.4*	26.1
CTV_Low	D_{max} (%)	106.5 ± 1.1	105.9 ± 1.2	106.4 ± 1.4	0.6	0.1	−0.5
	D_{mean} (%)	100.6 ± 0.2	100.2 ± 0.1	100.2 ± 0.1	0.4*	0.4*	0.0
	Mean ID (Gy.ml)	5111.7 ± 2913.9	5103.5 ± 2905.0	5092.6 ± 2905.9	0.3*	0.4*	0.0
CTV_High	D_{max} (%)	104.2 ± 1.2	104.5 ± 3.1	105.5 ± 1.4	−0.3	−1.2	−0.9
	D_{mean} (%)	100.7 ± 0.2	100.3 ± 0.2	100.3 ± 0.1	0.4*	0.4*	0.0
	Mean ID (Gy.ml)	1300.6 ± 1747.2	1297.0 ± 1742.0	1298.0 ± 1745.2	0.3*	0.4*	0.1
GTV_Low	D_{max} (%)	104.0 ± 1.5	105.4 ± 1.3	103.3 ± 1.2	−1.3	0.7	2.0*
	D_{mean} (%)	100.3 ± 0.2	100.4 ± 0.3	100.0 ± 0.1	−0.1	0.3*	0.4*
	Mean ID (Gy.ml)	1975.9 ± 1717.1	1978.1 ± 1719.7	1972.0 ± 1716.6	−0.1	0.2*	0.3*
GTV_High	D_{max} (%)	102.6 ± 1.1	103.9 ± 2.5	102.6 ± 1.1	−1.3	0.0	1.3
	D_{mean} (%)	100.6 ± 0.3	100.4 ± 0.5	100.0 ± 0.1	0.2	0.6*	0.4
	Mean ID (Gy.ml)	588.6 ± 926.9	589.6 ± 929.0	588.4 ± 921.9	−0.2	0.2*	0.0
Amygdala left	D_{max} (%)	91.4 ± 16.4	89.7 ± 15.9	93.5 ± 11.7	1.9	−2.2	−4.1
	D_{mean} (%)	79.7 ± 18.2	77.0 ± 17.5	85.0 ± 14.3	3.5	−6.2	−9.4*
	Mean ID (Gy.ml)	52.5 ± 26.6	50.8 ± 24.5	55.7 ± 22.7	3.3	−5.7	−8.8*
Amygdala right	D_{max} (%)	89.1 ± 16.1	87.6 ± 15.5	92.3 ± 11.5	1.7	3.5	−5.1
	D_{mean} (%)	79.1 ± 17.7	77.3 ± 16.8	84.4 ± 13.1	2.3	−6.3	−8.4*
	Mean ID (Gy.ml)	60.7 ± 26.4	59.3 ± 26.1	64.4 ± 24.6	2.4	−5.7	−7.9*
Brainstem	D_{max} (%)	102.1 ± 0.6	102.6 ± 1.0	102.9 ± 0.9	−0.5	−0.8	−0.3
	D_{mean} (%)	74.8 ± 7.2	82.4 ± 6.0	77.3 ± 8.0	−9.2*	−3.2	6.6
	Mean ID (Gy.ml)	706.1 ± 130.2	777.4 ± 136.0	730.4 ± 144.7	−9.2*	−3.3	6.4
Cerebellum	D_{max} (%)	99.1 ± 4.7	101.1 ± 2.7	100.1 ± 4.3	−2.0	−1.0	1.0
	D_{mean} (%)	25.7 ± 3.4	55.5 ± 7.6	38.4 ± 4.3	−53.7*	−33.1*	44.5*
	Mean ID (Gy.ml)	1423.0 ± 309.0	3069.0 ± 692.0	2115.3 ± 376.9	−53.6*	−32.7*	45.1*
Chiasm	D_{max} (%)	91.2 ± 16.1	90.3 ± 15.4	91.8 ± 13.7	0.1	−0.7	−1.6
	D_{mean} (%)	73.0 ± 27.3	74.4 ± 24.7	78.4 ± 21.9	−1.9	−6.9	−5.1
	Mean ID (Gy.ml)	11.5 ± 6.0	11.6 ± 5.2	12.2 ± 5.1	−0.9	−5.7	−4.9
Circle of Willis	D_{max} (%)	102.6 ± 2.2	101.2 ± 2.7	96.8 ± 20.1	1.4	6.0	4.5
	D_{mean} (%)	63.8 ± 24.3	68.7 ± 22.0	67.5 ± 26.2	−7.1*	−5.5	1.8
	Mean ID (Gy.ml)	85.6 ± 31.5	92.8 ± 29.6	90.5 ± 37.8	−7.8*	−5.4	2.5
Cochlea left	D_{max} (%)	21.0 ± 11.6	25.9 ± 6.6	17.0 ± 6.5	−18.9	23.5	52.5*
	D_{mean} (%)	12.0 ± 7.9	18.9 ± 4.2	13.2 ± 4.0	−36.5	−9.1	43.2*
	Mean ID (Gy.ml)	0.5 ± 0.3	0.8 ± 0.3	0.6 ± 0.2	−40.5	−20.7	33.3*
Cochlea right	D_{max} (%)	22.8 ± 17.9	24.5 ± 6.7	17.8 ± 6.9	−6.9	28.1	37.6*
	D_{mean} (%)	13.3 ± 10.9	18.6 ± 4.2	13.5 ± 4.5	−28.5	−1.5	37.8*
	Mean ID (Gy.ml)	0.5 ± 0.4	0.7 ± 0.2	0.5 ± 0.2	−28.6	0.0	40.0*
Hippocampus left	D_{max} (%)	101.1 ± 0.5	101.1 ± 0.7	101.4 ± 0.5	0.0	−0.3	−0.3
	D_{mean} (%)	84.5 ± 10.5	79.6 ± 11.7	89.2 ± 7.9	6.2*	−5.3	−10.8*
	Mean ID (Gy.ml)	109.9 ± 37.9	103.6 ± 37.5	116.1 ± 37.8	6.1*	−5.3	−10.8*
	$D_{40\%}$ (%)	87.8 ± 13.2	84.9 ± 11.8	91.1 ± 8.0	3.4	−4.4	−7.5
Hippocampus right	Dmax	97.5 ± 12.0	98.3 ± 8.0	99.5 ± 6.1	−0.8	−2.0	−1.2
	Dmean	79.6 ± 12.4	76.3 ± 11.7	86.4 ± 8.9	4.3	−7.9	−11.7*
	Mean ID (Gy.ml)	110.1 ± 35.3	102.5 ± 33.6	119.6 ± 37.4	7.4	−7.9	−14.3*
	$D_{40\%}$ (%)	79.4 ± 14.0	78.3 ± 13.4	87.5 ± 8.9	1.4	−9.3	−10.5
Hypothalamus left	D_{max} (%)	100.9 ± 0.3	102.0 ± 1.0	101.1 ± 0.5	−1.1	−0.2	0.9
	D_{mean} (%)	97.8 ± 7.8	97.8 ± 6.1	97.2 ± 6.4	0.0	0.6*	0.6
	Mean ID (Gy.ml)	11.3 ± 5.6	11.3 ± 5.5	11.2 ± 5.6	0.0	0.9*	0.9

Table 1 (*continued*)

VOI	Parameter	PBS-PT	IMRT	VMAT	PBS-PT vs. IMRT (%)	PBS-PT vs. VMAT (%)	IMRT vs. VMAT (%)
Hypothalamus right	D_{max} (%)	100.7 ± 1.1	101.7 ± 2.1	100.5 ± 2.9	−1.0	0.2	1.2*
	D_{mean} (%)	97.8 ± 8.1	97.9 ± 6.3	97.1 ± 7.0	−0.1	0.7	0.8
	Mean ID (Gy.ml)	11.6 ± 5.5	11.6 ± 5.4	11.6 ± 5.5	0.0	0.0	0.0
Lacrimal gland left	D_{max} (%)	6.6 ± 17.1	8.6 ± 7.2	18.5 ± 6.9	−23.3*	−64.3*	−53.5*
	D_{mean} (%)	2.6 ± 7.2	5.7 ± 4.5	22.2 ± 27.0	−54.4*	−88.3*	−74.3*
	Mean ID (Gy.ml)	0.4 ± 1.2	0.9 ± 0.8	3.8 ± 5.6	−57.6*	−89.5*	−75.2*
Lacrimal gland right	D_{max} (%)	1.3 ± 3.2	7.6 ± 5.8	17.7 ± 6.4	−82.9*	−92.7*	−57.1*
	D_{mean} (%)	0.3 ± 0.8	5.3 ± 4.3	13.5 ± 6.1	−94.3*	−97.8*	−60.7*
	Mean ID (Gy.ml)	0.0 ± 0.1	0.8 ± 0.5	2.1 ± 0.8	−95.8*	−98.4*	−61.9*
Lens left	D_{max} (%)	0.4 ± 1.3	4.1 ± 2.5	10.9 ± 4.8	−90.2*	−96.3*	−62.4*
	D_{mean} (%)	0.2 ± 0.6	3.7 ± 2.1	9.3 ± 4.0	−94.6*	−97.8*	−60.2*
	Mean ID (Gy.ml)	0.0 ± 0.0	0.3 ± 0.2	0.8 ± 0.4	−100.0*	−100.0*	−62.5*
Lens right	D_{max} (%)	0.0 ± 0.0	3.9 ± 2.1	11.1 ± 5.0	−100.0*	−100.0*	−64.9*
	D_{mean} (%)	0.0 ± 0.0	3.6 ± 1.9	9.4 ± 4.1	−100.0*	−100.0*	−61.7*
	Mean ID (Gy.ml)	0.0 ± 0.0	0.3 ± 0.1	0.7 ± 0.2	−100.0*	−100.0*	−58.2*
Normal brain (brain minus PTV)	D_{max} (%)	100.7 ± 0.5	103.3 ± 1.6	102.3 ± 1.5	−2.5*	−1.6*	1.0
	D_{mean} (%)	30.0 ± 8.6	46.3 ± 10.0	44.6 ± 9.1	−35.2*	−32.7*	3.8
	Mean ID (Gy.ml)	12211.7 ± 3402.8	18846.4± 3924.7	18226.7± 3887.2	−35.2*	−33.0*	3.4
Optic globe left	D_{max} (%)	8.6 ± 23.6	12.0 ± 14.8	22.9 ± 12.4	−28.3*	−62.4*	−47.6*
	D_{mean} (%)	1.0 ± 3.2	5.2 ± 4.4	13.9 ± 6.8	−80.8*	−92.8*	−62.6*
	Mean ID (Gy.ml)	3.3 ± 10.4	16.1 ± 14.3	42.3 ± 21.4	−79.5*	−92.2*	−61.9*
Optic globe right	D_{max} (%)	2.0 ± 3.5	8.9 ± 6.8	20.5 ± 0.8	−77.5*	−90.2*	−56.6*
	D_{mean} (%)	0.1 ± 0.2	4.7 ± 0.2	13.2 ± 6.7	−97.9*	−99.2*	−64.4*
	Mean ID (Gy.ml)	0.3 ± 0.6	14.8 ± 11.6	40.3 ± 22.4	−98.2*	−99.3*	−63.3*
Optic nerve left	D_{max} (%)	65.4 ± 42.4	58.8 ± 38.2	61.3 ± 35.5	11.2	6.7	−4.1
	D_{mean} (%)	20.4 ± 22.6	24.1 ± 20.0	30.5 ± 19.2	−15.4	−33.1*	−21.0*
	Mean ID (Gy.ml)	2.5 ± 2.4	3.2 ± 1.9	4.2 ± 1.9	−21.9	−40.5	−23.8*
Optic nerve right	D_{max} (%)	62.9 ± 38.7	56.3 ± 38.8	59.0 ± 36.0	11.7	6.6	−4.6
	D_{mean} (%)	15.7 ± 22.3	22.1 ± 19.6	28.7 ± 19.4	−29.0	−45.3*	−23.0*
	Mean ID (Gy.ml)	1.9 ± 2.1	2.9 ± 1.8	3.9 ± 1.8	−34.5	−51.3*	−25.6*
Parotid left	D_{max} (%)	0.6 ± 1.8	18.2 ± 6.7	9.7 ± 2.6	−96.7*	−93.8*	87.6*
	D_{mean} (%)	0.0 ± 0.0	5.9 ± 1.9	5.5 ± 1.8	−100.0*	−100.0*	7.3
	Mean ID (Gy.ml)	0.0 ± 0.0	25.6 ± 11.9	25.5 ± 19.8	−100.0*	−100.0*	0.4
Parotid right	D_{max} (%)	0.3 ± 0.7	16.7 ± 5.9	8.9 ± 2.0	−98.2*	−96.6*	87.6*
	D_{mean} (%)	0.0 ± 0.0	5.7 ± 2.1	5.1 ± 1.4	−100.0*	−100.0*	11.8
	Mean ID (Gy.ml)	0.0 ± 0.0	24.6 ± 13.3	22.6 ± 13.2	−100.0*	−100.0*	8.8
Pituitary	D_{max} (%)	68.9 ± 32.5	63.2 ± 34.5	60.8 ± 37.4	9.0	13.3	3.9
	D_{mean} (%)	54.5 ± 41.2	53.6 ± 39.6	53.9 ± 39.4	1.7	1.1	0.6
	Mean ID (Gy.ml)	11.4 ± 15.2	11.3 ± 14.9	11.4 ± 14.9	0.9	0.0	−0.9
Skin	D_{max} (%)	38.7 ± 25.0	46.7 ± 6.0	47.5 ± 9.7	−17.1	−18.5	−1.7
	D_{mean} (%)	13.8 ± 19.2	9.0 ± 2.8	8.0 ± 2.2	53.3	72.5	12.5
	Mean ID (Gy.ml)	701.5 ± 774.4	612.2 ± 357.3	553.6 ± 343.3	14.6	26.7	10.6
Spinal cord	D_{max} (%)	54.8 ± 11.7	51.2 ± 19.4	46.1 ± 22.1	7.0	18.9	11.1
	D_{mean} (%)	13.1 ± 8.3	12.4 ± 7.8	8.9 ± 6.5	5.6	47.2*	39.3*
	Mean ID (Gy.ml)	22.2 ± 13.8	21.9 ± 14.2	15.3 ± 11.1	1.4	45.1*	43.1*
Supratentorial	D_{max} (%)	103.2 ± 1.6	103.9 ± 1.6	103.4 ± 1.1	−0.7	−0.2	0.5
	D_{mean} (%)	39.8 ± 11.9	52.2 ± 11.9	50.2 ± 11.3	−23.8*	−20.7*	4.0
	Mean ID (Gy.ml)	36821.3± 65329.3	47163.9± 81511.6	46058.0 ± 80876.5	−21.9*	−20.1*	2.4
SVZ left	D_{max} (%)	99.0 ± 5.3	99.2 ± 5.8	98.6 ± 6.8	−0.2	0.4	0.6
	D_{mean} (%)	76.5 ± 11.3	75.5 ± 11.9	80.5 ± 10.7	1.3	−5.0*	−6.2*
	Mean ID (Gy.ml)	192.7 ± 159.8	193.6 ± 167.6	202.0 ± 164.8	−0.5	−4.6*	−4.2*
SVZ right	D_{max} (%)	93.6 ± 12.3	95.5 ± 11.1	96.1 ± 8.3	−2.0*	−2.6*	−0.6
	D_{mean} (%)	73.7 ± 11.9	73.3 ± 11.9	78.9 ± 10.5	0.5	−6.6*	−7.1
	Mean ID (Gy.ml)	177.3 ± 148.3	179.5 ± 156.8	188.4 ± 153.0	−1.2	−5.9*	−4.7
Temporal lobe left	D_{max} (%)	101.0 ± 3.7	100.9 ± 5.0	101.1 ± 4.1	0.1	−0.1	−0.2
	D_{mean} (%)	49.0 ± 19.5	50.5 ± 13.4	58.8 ± 19.9	−3.0*	−16.7	−14.1*
	Mean ID (Gy.ml)	2444.9 ± 1406.6	2455.2 ± 899.2	2819.5 ± 1211.3	−0.4*	−13.3	−12.9*
	V_{20Gy} (%)	107.4 ± 37.7	134.7 ± 55.6	177.8 ± 42.4	−20.3	−39.6*	−24.2*
Temporal lobe right	D_{max} (%)	97.0 ± 10.1	97.7 ± 8.3	99.7 ± 5.8	−0.7	−2.7	−2.0*
	D_{mean} (%)	43.1 ± 14.0	50.4 ± 14.1	63.3 ± 12.5	−14.5*	−31.9*	−20.4*
	Mean ID (Gy.ml)	4621.6 ± 8441.5	5420.9 ± 9931.5	6588.9 ± 51.5	−14.7*	−29.9*	−17.7*
Thalamus left	V_{20Gy} (%)	104.2 ± 36.5	137.4 ± 51.5	177.0 ± 42.0	−24.2*	−41.1*	−22.4*
	D_{max} (%)	101.1 ± 0.4	102.5 ± 1.2	101.9 ± 0.6	−1.4	−0.8*	0.6
	D_{mean} (%)	96.5 ± 3.6	96.2 ± 3.8	95.3 ± 5.6	0.3	1.3	0.9
	Mean ID (Gy.ml)	214.8 ± 44.8	214.6 ± 47.3	211.6 ± 42.6	0.1	1.5	1.4
Thalamus right	D_{max} (%)	101.2 ± 0.4	102.4 ± 1.1	102.1 ± 0.8	−1.2	−0.9	0.3
	D_{mean} (%)	93.4 ± 8.0	93.5 ± 6.4	94.8 ± 4.6	−0.1	−1.5	−1.4
	Mean ID (Gy.ml)	211.2 ± 44.9	211.8 ± 46.0	214.3 ± 44.4	−0.3	−1.4	−1.2
TMJ left	D_{max} (%)	9.7 ± 8.7	16.5 ± 8.0	12.0 ± 4.4	−44.6*	−19.2	45.8*
	D_{mean} (%)	1.0 ± 1.2	9.9 ± 3.6	8.5 ± 2.6	−89.9*	−88.2*	16.5
	Mean ID (Gy.ml)	0.9 ± 1.3	8.1 ± 3.9	7.0 ± 3.3	−88.7*	−87.0*	15.7

Table 1 (*continued*)

VOI	Parameter	PBS-PT	IMRT	VMAT	PBS-PT vs. IMRT (%)	PBS-PT vs. VMAT (%)	IMRT vs. VMAT (%)
TMJ right	D_{max} (%)	10.7 ± 11.8	18.0 ± 8.7	12.7 ± 4.6	−40.6[*]	−15.7	41.7[*]
	D_{mean} (%)	1.3 ± 1.8	9.7 ± 4.2	8.6 ± 2.6	−86.1[*]	−83.8[*]	16.2
	Mean ID (Gy.ml)	1.1 ± 1.6	7.9 ± 4.5	6.8 ± 3.3	−86.0[*]	−83.8[*]	16.2
Values are given as mean relative dose with standard deviations in percentage (%):							
– Primary phase	(PTV_Low, CTV_Low, GTV_Low)			24 Gy			
– Boost phase	(PTV_High, CTV_High, GTV_High)			16 Gy			= 100%
– Organs at risk	All other VOI			40 Gy			

Abbreviations: VOI, volume of interest; PTV, planning target volume; D_{max}, maximum dose of VOI; D_{mean}, average dose of VOI; D_{min}, minimum dose of VOI; ID, integral dose (D_{mean} × volume); $V_{90\%}$, percentage of PTV receiving a minimum of 90% of the prescribed dose; $V_{95\%}$, percentage of PTV receiving a minimum of 95% of the prescribed dose; $V_{100\%}$, percentage of PTV receiving a minimum of 100% of the prescribed dose; HI, homogeneity index (($D_{5\%} - D_{95\%}$)/prescribed dose × 100); IC, inhomogeneity coefficient (($D_{max} - D_{min}$)/D_{mean}); CTV, clinical target volume; GTV, gross tumour volume; SVZ, subventricular zone; TMJ, temporomandibular joint.

[*] Indicates statistically significant differences (p < 0.017) in the Friedman test with the Bonferroni posttest.
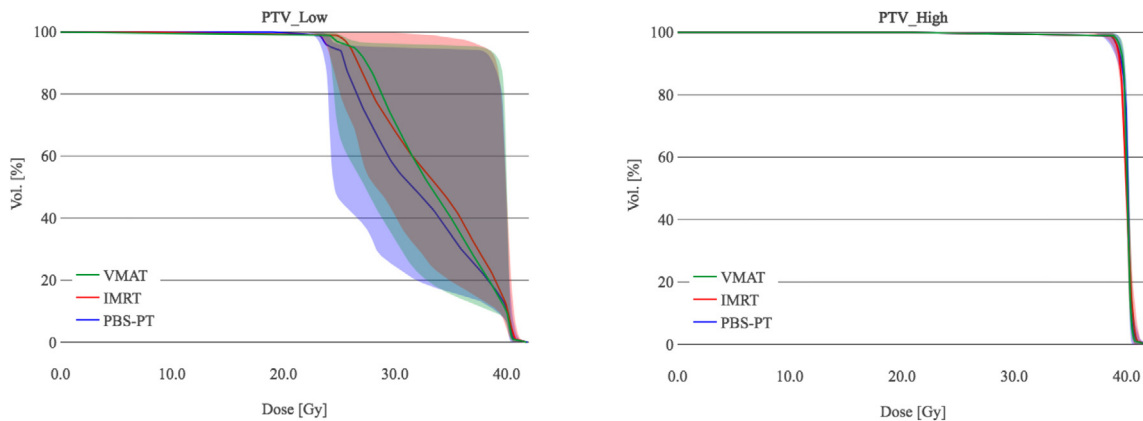

Fig. 2. Cumulative dose-volume histograms (DVH) (mean dose, n = 11) with range for PTV coverage with PBS-PT, IMRT and VMAT plans.

35.5–41.6 Gy). However, the statistically significant difference to IMRT and VMAT could be seen on D_{mean} (−53.7%, −33.1%) and ID (-53.6%, −32.7%), favoring the proton over the photon plans. Between IMRT and VMAT, the latter seems dosimetrically beneficial (−44.5% Dmean; −45.1% ID) regarding cerebellum dose exposure (Fig. 3).

Compared to IMRT and VMAT, PBS-PT showed the following statistically significant reduction in:

- temporal lobe – D_{mean} (−14.5%, −31.9%), ID (−14.7%, −29.9%), V_{20Gy} (−24.2%, −41.1%) on the right side. Moreover, the left temporal lobe dose sparing was higher with protons (PBS-PT D_{mean}, ID better than IMRT; PBS-PT V_{20Gy} better than VMAT). Compared to VMAT, IMRT seems advantageous in both lobes.

- subventricular zone (SVZ) – maximum dose (D_{max}) (−2.0%, −2.6%) on the right side. Furthermore, VMAT had the least dose sparing in comparison to the other two modalities (PBS-PT D_{mean} and ID better spared on both sides, while IMRT D_{mean} and ID on the left side).

Neurons and glial cells are produced from neurogenic stem cells located in the SVZ of the lateral ventricles and the subgranular zone of the hippocampal gyrus. These areas form part of the limbic system, located in the temporal lobe. They have important roles in various aspects of memory and emotional learning [23] and are very susceptible to radiation-induced damage, particularly in the developing tissues of young patients [24]. A dose-dependent thinning of the cerebral cortex was described, with a pronounced effect
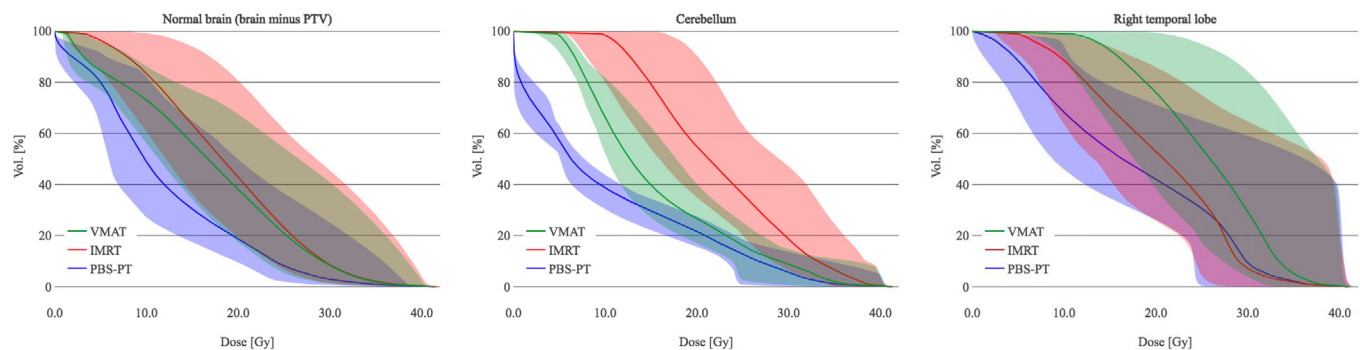

Fig. 3. Cumulative DVH (mean dose, n = 11) with range for (N)OAR with a significant dose difference for PBS-PT compared to photons.

in the temporal lobes and limbic cortex [25]. The proposed dose constraint for the hippocampi is currently $D_{40\%} \leq 7.3$ Gy to avoid memory loss [10]. Prospective data demonstrate not only a significant association between increasing dose to the hippocampus and temporal lobes and decline in neurocognitive skills following cranial irradiation [26], but also with the dose and volume of the irradiated healthy brain and the IQ [27]. Age was also an important determinant of impact on IQ, with younger children being more sensitive to neurocognitive effects of RT [11,28]. Especially in this population, a decrease in IQ, processing speed, and fine motor skills have been reported after chemoradiation, with memory impairment associated with a $D_{max} > 30$ Gy to the temporal lobe [29]. When normal tissue volumes such as the supratentorial brain or temporal lobes receive less of the low and intermediate doses [28], it resulted in clinically significant higher IQ scores for patients with intracranial tumors [30].

3.2.2. NOAR of cerebrovascular function

PBS-PT allowed for a statistically significant difference of −7.1% D_{mean} and −7.8% ID of the Willis' circle, when compared to IMRT.

El-Fayech et al. reported that at 45 years of age, the cumulative stroke incidence was 11.3% in patients who had received $D_{mean} \geq 10$ Gy to the Willis' circle as children, compared with 1% expected from general population data [31]. In our cohort, the D_{mean} applied to the Willis' circle was 25.5 Gy (range, 10.3–39.7 Gy) for PBS-PT, 27.5 Gy (range, 14.1–39.7 Gy) for IMRT and 27.0 Gy (range, 2.5–39.4 Gy) for VMAT. Nevertheless, the ALARA concept seems to play an important role on the potential of decreasing the likelihood of vascular sequelae: an association of 5% stroke hazard increase per 1 Gy (D_{mean}) mainly to the Willis' circle was estimated in a longitudinal data set of >10,000 cancer survivors [32], thus showing a dose-dependent effect (almost 30-fold higher risk of stroke after cranial RT than the general population) [31].

3.2.3. NOAR of neuroendocrine function

Regarding the hypothalamic-pituitary axis, only the VMAT D_{mean} and ID of the left hypothalamus were significantly lower (−0.6% and −0.9%, respectively) comparing with PBS-PT and D_{max} (−1.2%) comparing with IMRT.

Even low dose on the hypothalamic-pituitary axis influences the occurrence of endocrinopathy [19]. Pai et al. reported that $D_{mean} < 20$ Gy(RBE) to the hypothalamus was associated with endocrinopathy, even though this association was only found for a $D_{min} > 50$ Gy(RBE) for the pituitary gland [33]. Chemaitilly et al. identified an association between luteinizing hormone/follicle-stimulating hormone deficiencies already with 22 Gy D_{mean} to the pituitary gland and hypothalamus on a lifetime cohort study of adult survivors of childhood cancers [34]. In our cohort, the lowest pituitary D_{mean} was achieved with IMRT, with 21.4 Gy (range, 6.2–40.1 Gy), while PBS-T 21.8 Gy (range, 2.6–41.4 Gy) and VMAT 21.6 Gy (range, 1.7–40.0 Gy). Moreover, 30 Gy D_{mean} to the pituitary gland might cause growth hormone deficiency in ≤ 30% of patients, with 30–50 Gy affecting 50–100% [35].

3.2.4. Other NOAR function

3.2.4.1. Vision.
The lacrimal glands, lenses and optic globes could be better spared with PBS-PT, comparing with photons (in D_{max}, D_{mean}, ID); yet better with IMRT, when compared to VMAT. The risk for keratoconjunctivitis sicca could be avoided, as in all modalities D_{mean} of each lacrimal gland was ≤25 Gy [10]. The potential for cataract is low, as $D_{0.03cc}$ of each lens was ≤10 Gy [10], even <6 Gy [15], according to the recommended constraints.

The risk for neuropathic complication is extremely low, considering the low optic nerve dose presented in every RT modality. The lowest optic nerve D_{max} was achieved with IMRT. However, a statistically significant difference was reached in favor of IMRT (in D_{mean} and ID) only by comparing it with VMAT.

3.2.4.2. Audition.
To avoid tinnitus, the D_{mean} of the cochleae should be ≤32 Gy [10], which was possible with all three techniques. The lowest cochlear D_{mean} was achieved with PBS-PT. However, a statistically significant difference was reached (in D_{max}, D_{mean}, ID) only by comparing IMRT with VMAT, in favor of the latter.

3.2.5. Other potential late toxicity

3.2.5.1. Radionecrosis.
The D_{mean} applied to the brainstem was 29.9 Gy (range, 24.9–34.3 Gy) for PBS-PT, 33.0 Gy (range, 28.7–36.3 Gy) for IMRT and 30.9 Gy (range, 28.7–36.6 Gy) for VMAT. According to Uy et al., exceeding the 30 Gy D_{mean} might increase the incidence of severe brainstem necrosis in 3% [36]. Considering our pediatric cohort, a lower threshold should be taken into account. The lowest brainstem dose exposure was achieved with PBS-PT in all its dose-metrics. However, a statistically significant difference was reached only when compared to IMRT (−9.2% D_{mean} and ID).

With the applied dose to the temporal lobes (3.2.1., Table 1), the risk for necrosis is very low.

3.2.5.2. Myelopathy.
Even though the spinal cord D_{max} of this cohort has not exceeded 30.2 Gy (IMRT) – therefore, not expecting the risk of myelopathy –, the highest spinal cord sparing was achieved with VMAT. Compared with PBS-PT and IMRT, VMAT presented reduced D_{mean} (−47.2%, −39.3%) and ID (−45.1%, −43.1%).

3.2.5.3. Alopecia.
No permanent alopecia is expected, as $D_{0.03cc}$ of the skin was ≤25 Gy [10].

3.2.5.4. Risk for secondary malignancy.
Healthy brain tissue, as a potential risk area for secondary malignancy, could be spared mainly with protons: D_{mean} 12.0 Gy (range, 8–20.5 Gy) for PBS-PT, 18.5 Gy (range, 12.9–28.2 Gy) for IMRT and 17.9 Gy (range, 14.11–25.0 Gy) for VMAT. Despite no clinical proof of a sequelae difference regarding this dose level to the pediatric brain, it is known that even relatively low doses of radiation, once perceived as being "safe", may increase the probability of the development of secondary cancers [37]. Therefore, the ALARA concept should be followed. Moreover, an ID reduction, as seen in the proton plans, is expected to result in a lower rate of secondary tumor induction after treatment [38]. Compared to IMRT and VMAT, PBS-PT showed the following statistically significant differences:

- normal brain (brain without PTV) – D_{max} (−2.5%, −1.6%), D_{mean} (−35.2%, −32.7%) and ID (−35.2%, −33.0%, respectively);
- supratentorial brain – D_{mean} (−23.8%, −20.7%) and ID (−21.9%, −20.1%)
- parotid glands – D_{max} (left: −96.7%, −93.8%; right: −98.2%, −96.6%), D_{mean} (−100.0%, −100.0%) and ID (−100.0%, −100.0%).

The dose to the parotid glands is way below the recommended 20 Gy in every modality, meaning that the expected xerostomia will be below 20% [39]. The PBS-PT dose is otherwise close to 0.0 Gy in every dose-metric, similar to the lenses and temporo-mandibular joints. In comparison, these healthy tissues would be susceptible to develop a secondary malignancy if this long-term survivor cohort would have been treated with photons.

3.3. Comparative evaluation of treatment plans

RT planning with steep dose gradient is required to better spare the NOAR. Effective immobilization and accurate radiation delivery methods are therefore crucial to provide the higher degree of

set-up reproducibility required. This varies with the immobilization type used and compliance of the patient. For PBS-PT plans, a 4 mm CTV-PTV margin for a bite-block immobilization system was applied at PSI. At Inselspital, a 3 mm margin for a frameless thermoplastic mask would have been used instead. On the one hand, the lowest margin could be advantageous in comparison to the 4 mm margin by reducing the NOAR volume irradiated, mainly from the thalamus (Supplementary file Fig. A.1, light blue VOI). On the other hand, within this 1 mm difference, the number of NOAR included in the PTV_Low is the same. Furthermore, the 3 mm expansion on one TPS showed similar volume to the 4 mm expansion on the other TPS, thus being cursory to perform an analysis comparing both.

IMRT with dose painting has been shown in dosimetric comparisons to provide the most conformal photon treatment for WV-RT [40,41]. However, some studies raised concern about its possibility of creating a greater ID delivered mainly to the healthy brain [42]. Another sparing approach with photons is VMAT, with reduced treatment delivery time compared to conventional static field IMRT [43], which can be advantageous in a pediatric population. For future multiple-arc treatments, dynamic trajectory VMAT [27,44] might be a good study objective to provide further improvements in OAR sparing in IGCT, especially when PT is not available.

PT is an acknowledgeable technique for normal tissue sparing in pediatric cranial RT, with its predicted consistently lower doses to critical normal tissues and ID to the body [38] compared with photons [30]. Regarding WV-RT, MacDonald published one demonstrative case of WV-RT/TB in localized IGCT (WV = 23.4 Gy, boost 45 Gy) where intensity-modulated proton therapy with fine pencil beams (σ = 3 mm) allowed additional sparing over IMRT and conformal PT (passive scattering or PBS) [8]. Park presented a study with three WV-RT/TB cases (WV = 19.8 Gy, boost 30.6 Gy, normalized to get 100% of the D_p to 95% of the PTV), showing similar results [45]. Extrapolating from prospective studies [26,27], this approach might reduce the radiation-related late toxicity in survivors.

4. Conclusion

Taking into account the ALARA concept, PBS-PT can be a reasonable alternative to photons for IGCT, as it seems to reduce dose exposure to the surrounding NOAR while keeping good target coverage and better conformality. Otherwise, IMRT seems dosimetrically superior to VMAT regarding the NOAR sparing in WV-RT/TB. Overall, technical attempts to potentially reduce the dose- and volume-related side effects of treatment in long-term survivors should be pursued, ideally on prospectively assessing outcome.

Declarations of interest

None.

Authorship

All authors listed on the manuscript contributed to the experimental design, its implementation, or analysis and interpretation of the data. All authors were involved in the writing of the manuscript at draft and any revision stages, and have read and approved the final version.

Funding

Acknowledgments

Appendix A. Supplementary data

Supplementary data to this article can be found online at https://doi.org/10.1016/j.ctro.2019.01.002.

References

[1] Matsutani M, Sano K, Takakura K, Fujimaki T, Nakamura O, Funata N, et al. Primary intracranial germ cell tumors: a clinical analysis of 153 histologically verified cases. J Neurosurg 1997;86(3):446–55. https://doi.org/10.3171/jns.1997.86.3.0446.

[2] Weksberg DC, Shibamoto Y, Paulino AC. Bifocal intracranial germinoma: a retrospective analysis of treatment outcomes in 20 patients and review of the literature. Int J Radiat Oncol Biol Phys 2012;82(4):1341–51. https://doi.org/10.1016/j.ijrobp.2011.04.033.

[3] Echevarria ME, Fangusaro J, Goldman S. Pediatric central nervous system germ cell tumors: a review. Oncologist 2008;13(6):690–9. https://doi.org/10.1634/theoncologist.2008-0037.

[4] Brandes AA, Pasetto LM, Monfardini S. The treatment of cranial germ cell tumours. Cancer Treat Rev 2000;26(4):233–42. https://doi.org/10.1053/ctrv.2000.0169.

[5] Greenfield BJ, Jaramillo S, Abboud M, Mahajan A, Paulino AC, McGovern S, et al. Outcomes for pediatric patients with central nervous system germ cell tumors treated with proton therapy. Clin Transl Radiat Oncol 2016;1:9–14. https://doi.org/10.1016/j.ctro.2016.08.002.

[6] Bamberg M, Kortmann R-D, Calaminus G, Becker G, Meisner C, Harms D, et al. Radiation therapy for intracranial germinoma: results of the german cooperative prospective trials MAKEI 83/86/89. J Clin Onc 1999;17(8):2585. https://doi.org/10.1200/jco.1999.17.8.2585.

[7] Maity A, Shu HK, Janss A, Belasco JB, Rorke L, Phillips PC, et al. Craniospinal radiation in the treatment of biopsy-proven intracranial germinomas: twenty-five years' experience in a single center. Int J Radiat Oncol Biol Phys 2004;58 (4):1165–70. https://doi.org/10.1016/j.ijrobp.2003.08.028.

[8] MacDonald SM, Trofimov A, Safai S, Adams J, Fullerton B, Ebb D, et al. Proton radiotherapy for pediatric central nervous system germ cell tumors: early clinical outcomes. Int J Radiat Oncol Biol Phys 2011;79(1):121–9. https://doi.org/10.1016/j.ijrobp.2009.10.069.

[9] Odagiri K, Omura M, Hata M, Aida N, Niwa T, Ogino I, et al. Treatment outcomes, growth height, and neuroendocrine functions in patients with intracranial germ cell tumors treated with chemoradiation therapy. Int J Radiat Oncol Biol Phys 2012;84(3):632–8. https://doi.org/10.1016/j.ijrobp.2011.12.084.

[10] Lambrecht M, Eekers DBP, Alapetite C, Burnet NG, Calugaru V, Coremans IEM, et al. Radiation dose constraints for organs at risk in neuro-oncology; the European Particle Therapy Network consensus. Radiother Oncol 2018;128 (1):26–36. https://doi.org/10.1016/j.radonc.2018.05.001.

[11] Merchant TE, Kiehna EN, Li C, Xiong X, Mulhern RK. Radiation dosimetry predicts IQ after conformal radiation therapy in pediatric patients with localized ependymoma. Int J Radiat Oncol Biol Phys 2005;63(5):1546–54. https://doi.org/10.1016/j.ijrobp.2005.05.028.

[12] Eekers DBP, in 't Ven L, Deprez S, Jacobi L, Roelofs E, Hoeben A, et al. The posterior cerebellum, a new organ at risk? Clin Transl Radiat Oncol 2018;8:22–6. https://doi.org/10.1016/j.ctro.2017.11.010.

[13] Harrabi SB, Bougatf N, Mohr A, Haberer T, Herfarth K, Combs SE, et al. Dosimetric advantages of proton therapy over conventional radiotherapy with photons in young patients and adults with low-grade glioma. Strahlenther Onkol 2016;192(11):759–69. https://doi.org/10.1007/s00066-016-1005-9.

[14] Clinical Trials U. S. National Library of Medicine. (2011) Prospective Trial for the Diagnosis and Treatment of Intracranial Germ Cell Tumors (SIOP CNS GCT II). Available at https://clinicaltrials.gov/ct2/show/NCT01424839. (Accessed December 16, 2016).

[15] Scoccianti S, Detti B, Gadda D, Greto D, Furfaro I, Meacci F, et al. Organs at risk in the brain and their dose-constraints in adults and in children: a radiation oncologist's guide for delineation in everyday practice. Radiother Oncol 2015;114(2):230–8. https://doi.org/10.1016/j.radonc.2015.01.016.

[16] Frey K, Unholtz D, Bauer J, Debus J, Min CH, Bortfeld T, et al. Automation and uncertainty analysis of a method for in-vivo range verification in particle therapy. Phys Med Biol 2014;59(19):5903–19. https://doi.org/10.1088/0031-9155/59/19/5903.

[17] Weber DC, Lomax AJ, Rutz HP, Stadelmann O, Egger E, Timmermann B, et al. Spot-scanning proton radiation therapy for recurrent, residual or untreated intracranial meningiomas. Radiother Oncol 2004;71(3):251–8. https://doi.org/10.1016/j.radonc.2004.02.011.

[18] Pedroni E, Bacher R, Blattmann H, Bohringer T, Coray A, Lomax A, et al. The 200-MeV proton therapy project at the Paul Scherrer Institute: conceptual design and practical realization. Med Phys 1995;22(1):37–53. https://doi.org/10.1118/1.597522.

[19] Scheib S, Pedroni E. Dose calculation and optimization for 3D conformal voxel scanning. Radiat Environ Biophys 1992;31(3):251–6. https://doi.org/10.1007/BF01214833.

[20] Adeberg S, Harrabi SB, Bougatf N, Bernhardt D, Rieber J, Koerber SA, et al. Intensity-modulated proton therapy, volumetric-modulated arc therapy, and 3D conformal radiotherapy in anaplastic astrocytoma and glioblastoma: a dosimetric comparison. Strahlenther Onkol 2016;192(11):770–9. https://doi.org/10.1007/s00066-016-1007-7.

[21] D'Souza WD, Rosen II. Nontumor integral dose variation in conventional radiotherapy treatment planning. Med Phys 2003;30(8):2065–71. https://doi.org/10.1118/1.1591991.

[22] Gan HK, Bernstein LJ, Brown J, Ringash J, Vakilha M, Wang L, et al. Cognitive functioning after radiotherapy or chemoradiotherapy for head-and-neck cancer. Int J Radiat Oncol Biol Phys 2011;81(1):126–34. https://doi.org/10.1016/j.ijrobp.2010.05.004.

[23] Ajithkumar T, Price S, Horan G, Burke A, Jefferies S. Prevention of radiotherapy-induced neurocognitive dysfunction in survivors of paediatric brain tumours: the potential role of modern imaging and radiotherapy techniques. Lancet Oncol 2017;18(2):e91–e100. https://doi.org/10.1016/S1470-2045(17)30030-X.

[24] Athar BS, Paganetti H. Comparison of second cancer risk due to out-of-field doses from 6-MV IMRT and proton therapy based on 6 pediatric patient treatment plans. Radiother Oncol 2011;98(1):87–92. https://doi.org/10.1016/j.radonc.2010.11.003.

[25] Karunamuni R, Bartsch H, White NS, Moiseenko V, Carmona R, Marshall DC, et al. Dose-dependent cortical thinning after partial brain irradiation in high-grade glioma. Int J Radiat Oncol Biol Phys 2016;94(2):297–304. https://doi.org/10.1016/j.ijrobp.2015.10.026.

[26] Redmond KJ, Mahone EM, Terezakis S, Ishaq O, Ford E, McNutt T, et al. Association between radiation dose to neuronal progenitor cell niches and temporal lobes and performance on neuropsychological testing in children: a prospective study. Neuro-Oncol 2013;15(3):360–9. https://doi.org/10.1093/neuonc/nos303.

[27] Agbahiwe H, Rashid A, Horska A, Mahone EM, Lin D, McNutt T, et al. A prospective study of cerebral, frontal lobe, and temporal lobe volume and neuropsychological performance in children with primary brain tumors treated with cranial radiation. Cancer 2017;123(1):161–8. https://doi.org/10.1002/cncr.30313.

[28] Merchant TE, Hua C, Shukla H, Ying X, Nill S, Oelfke U. Proton versus photon radiotherapy for common pediatric brain tumors: Comparison of models of dose characteristics and their relationship to cognitive function. Pediatr Blood Cancer 2008;51(1):110–7. https://doi.org/10.1002/pbc.21530.

[29] Armstrong GT, Jain N, Liu W, Merchant TE, Stovall M, Srivastava DK, et al. Region-specific radiotherapy and neuropsychological outcomes in adult survivors of childhood CNS malignancies. Neuro Oncol 2010;12(11):1173–86. https://doi.org/10.1093/neuonc/noq104.

[30] Leung HW, Chan AL, Chang MB. Brain dose-sparing radiotherapy techniques for localized intracranial germinoma: case report and literature review of modern irradiation. Cancer Radiother 2016;20(3):210–6. https://doi.org/10.1016/j.canrad.2016.02.007.

[31] El-Fayech C, Haddy N, Allodji RS, Veres C, Diop F, Kahlouche A, et al. Cerebrovascular diseases in childhood cancer survivors: role of the radiation dose to willis circle arteries. Int J Radiat Oncol Biol Phys 2017;97(2):278–86. https://doi.org/10.1016/j.ijrobp.2016.10.015.

[32] Mueller S, Sear K, Hills NK, Chettout N, Afghani S, Gastelum E, et al. Risk of first and recurrent stroke in childhood cancer survivors treated with cranial and cervical radiation therapy. Int J Radiat Oncol Biol Phys 2013;86(4):643–8. https://doi.org/10.1016/j.ijrobp.2013.03.004.

[33] Pai HH, Thornton A, Katznelson L, Finkelstein DM, Adams JA, Fullerton BC, et al. Hypothalamic/pituitary function following high-dose conformal radiotherapy to the base of skull: demonstration of a dose-effect relationship using dose-volume histogram analysis. Int J Radiat Oncol Biol Phys 2001;49:1079–92.

[34] Chemaitilly W, Li Z, Huang S, Ness KK, Clark KL, Green DM, et al. Anterior hypopituitarism in adult survivors of childhood cancers treated with cranial radiotherapy: a report from the St Jude Lifetime Cohort study. J Clin Oncol 2015;33(5):492–500. https://doi.org/10.1200/JCO.2014.56.7933.

[35] Darzy KH, Shalet SM. Hypopituitarism following radiotherapy. Pituitary 2009;12(1):40–50. https://doi.org/10.1007/s11102-008-0088-4.

[36] Uy NW, Woo SY, Teh BS, Mai WY, Carpenter LS, Chiu JK, et al. Intensity-modulated radiation therapy (IMRT) for meningioma. Int J Radiat Oncol Biol Phys 2002;53:1265–70. https://doi.org/10.1016/S0360-3016(02)02823-7.

[37] Stewart FA, Akleyev AV, Hauer-Jensen M, Hendry JH, Kleiman NJ, MacVittie TJ, et al. ICRP PUBLICATION 118: ICRP Statement on Tissue Reactions and Early and Late Effects of Radiation in Normal Tissues and Organs — Threshold Doses for Tissue Reactions in a Radiation Protection Context. Ann ICRP 2012;41(1–2):1–322. https://doi.org/10.1016/j.icrp.2012.02.001.

[38] Schneider U, Lomax A, Pemler P, Besserer J, Ross D, Lombriser N, et al. The impact of IMRT and proton radiotherapy on secondary cancer incidence. Strahlenther Onkol 2006;182(11):647–52. https://doi.org/10.1007/s00066-006-1534-8.

[39] Brodin NP, Tome WA. Revisiting the dose constraints for head and neck OARs in the current era of IMRT. Oral Oncol 2018;86:8–18. https://doi.org/10.1016/j.oraloncology.2018.08.018.

[40] Raggi E, Mosleh-Shirazi MA, Saran FH. An evaluation of conformal and intensity-modulated radiotherapy in whole ventricular radiotherapy for localised primary intracranial germinomas. Clin Oncol (R Coll Radiol) 2008;20(3):253–60. https://doi.org/10.1016/j.clon.2007.12.011.

[41] Yang JC, Terezakis SA, Dunkel IJ, Gilheeney SW, Wolden SL. Intensity-modulated radiation therapy with dose painting: a brain-sparing technique for intracranial germ cell tumors. Pediatr Blood Cancer 2016;63(4):646–51. https://doi.org/10.1002/pbc.25867.

[42] Ruben JD, Davis S, Evans C, Jones P, Gagliardi F, Haynes M, et al. The effect of intensity-modulated radiotherapy on radiation-induced second malignancies. Int J Radiat Oncol Biol Phys 2008;70(5):1530–6. https://doi.org/10.1016/j.ijrobp.2007.08.046.

[43] Teoh M, Clark CH, Wood K, Whitaker S, Nisbet A. Volumetric modulated arc therapy: a review of current literature and clinical use in practice. Br J Radiol 2011;84(1007):967–96. https://doi.org/10.1259/bjr/22373346.

[44] Fix MK, Frei D, Volken W, Terribilini D, Mueller S, Elicin O, et al. Part 1: optimization and evaluation of dynamic trajectory radiotherapy. Med Phys 2018. https://doi.org/10.1002/mp.13086.

[45] Park J, Park Y, Lee SU, Kim T, Choi Y-K, Kim J-Y. Differential dosimetric benefit of proton beam therapy over intensity modulated radiotherapy for a variety of targets in patients with intracranial germ cell tumors. Radiat Oncol 2015;10(1). https://doi.org/10.1186/s13014-015-0441-5.